

Research Paper

Antibacterial Activities of the CuO/ZnO Nanocomposite Grown on Silica Extracted from Bagasse Ash

Yirgalem Negash, Birhanu Tolosa, Tegene Bantewesen, Gebisa Bekele*

Department of Material Science and Engineering, Adama Science & Technology University, P. O. Box 1888, Adama, Ethiopia

Article Info

Article History:

Received 07 September
2020

Received in revised form
02 December 2020

Accepted 14 December
2020

Keywords:

Sugarcane bagasse ash

Sol-gel

CuO/ZnO

Silica

Antibacterial activities

Abstract

Nano-scaled Zinc oxide and Copper oxide semiconductors have been widely used as antibacterial agents because of low cost and non-toxicity, but high agglomeration and high electron-holes recombination rates hinder their performances. In this work, we synthesized silica-supported CuO/ZnO and CuO/ZnO bare nanocomposites by the sol-gel technique. The antibacterial activities of both nanocomposites have compared on Gram-negative (*E. coli*) and Gram-positive (*S. aureus*) bacteria. The average crystal sizes of CuO/ZnO bare is 16.3 nm, and silica-supported CuO/ZnO is 29.1 nm as calculated from XRD data. Moreover, SEM results showed that there was no agglomeration in silica-supported CuO/ZnO due to the presence of silica. When antibacterial activities of both nanocomposites were tested by using the agar diffusion method, silica-supported CuO/ZnO showed an inhibition zone of 51% for *Staphylococcus aureus* and 53% for *Escherichia coli* compared with that of CuO/ZnO bare. Therefore, silica-supported CuO/ZnO nanocomposite is a promising antibacterial agent because of its low cost, non-toxicity, and good antibacterial properties.

1. Introduction

Nano-scaled semiconductors are materials with a size in the range of 1-100 nm, narrow size distribution, high agglomeration, and a high dispersion (Lines, 2008). Due to such novel properties of nanomaterials, they are utilized in different applications such as wastewater treatment, paints, cosmetics displays, medicine, batteries, catalysis, gas sensor, food engineering, and agriculture (Arivalagan et al., 2011). In developing countries like Ethiopia, waste management practices are so poor that it is common to hear news about widespread of infectious diseases. For instance, Ethiopia have a sufficient amount of water resources in East Africa. The two sources of water in Ethiopia are surface and subsurface water: Surface water is around one hundred twenty-four billion cubic meters and

underground water is thirty million cubic meters (Ademe et al., 2014). However, the water quality is deteriorated due to improper management of industrialization, urbanization, organic water pollutants, inorganic water pollutants, and agricultural waste (Sharma et al., 2017; Inyinbor et al., 2018; Mia et al., 2019). Drinking such contaminated water causes diseases like Cholera, Dracunculiasis, Typhoid fever, Diarrhea, Ulcers, Hepatitis, and Arsenicosis (Fazal-ur-Rehman, 2019; Hopkins et al., 2019).

Starting from the discovery of Penicillin in 1928, a complete transformation in global health and life expectancy has been observed. But, the appearance of antibiotics resistance bacteria has awoken the research communities to figure out antibacterial agents that able

* Corresponding author, e-mail: gebisabek12@gmail.com

<https://doi.org/10.20372/ejssdastu.v8.i1.2021.319>

to treat antibiotic resistance bacteria. Due to the evolution of drug resistance in pathogenic bacteria, the normally treated illnesses yesterday are becoming fatal today. To tackle the challenges that have been caused by antibiotic resistance bacteria, several schemes and approaches have proposed (Jan et al., 2019; Manyasree et al., 2017) like natural extracts (Shweta et al., 2015), adsorption (Ademiluyi et al., 2009), Ozonization (Nabi et al., 2006), photocatalysis (Claudia et al., 2019), and membrane filtration (Zioui et al., 2015). Among these methods, photocatalysis is easy to use, eco-friendly, and inexpensive. Photocatalysis mainly depends on the choice of metal oxide semiconductor that has the capability of creating electron-hole pair which generates free radicals to inhibit bacteria and degradation of dye (Sun et al., 2009). Nano-scaled metal oxide semiconductors used as photocatalyst are CuO (Manyasree et al., 2017), ZnO (Sun et al., 2009), WO₃ (Nandiyanto et al., 2017), MgO (Bandara et al: 2004) TiO₂ (Bandara et al: 2004) and Fe₂O₃ (Ahmmad et al., 2013).

ZnO is an n-type semiconductor, utilized broadly due to its high photocatalytic activity, non-toxic nature, inexpensive, hydrophilic property, excellent chemical and mechanical stability (Azmina et al., 2017). However, limitations of ZnO are confinement of ZnO, agglomeration, photo corrosion, the large bandgap energy (3.2 eV) (sherry et al., 2015; Saravanakkumar et al., 2019). CuO is a p-type semiconductor, narrow band gap energy (1.2 eV), low-electrical resistance values, inexpensive, and non-toxic. But, it has limitations like low photocatalytic activity that leads to the deficiency of charge transport inside CuO (Shirzadi et al., 2016; Anandan et al., 2007). Thus, CuO/ZnO nano-scaled semiconductor reduces the rate of electron-hole recombination and increases the lifetime of nanocomposites (Sakib et al., 2019; Widiarti et al., 2017), which leads to better photocatalytic properties. The main challenge of CuO/ZnO nanocomposite is agglomeration, poor catalytic efficiency, and difficulty in separation of nanocomposite from solution after use (Azmina et al., 2017), (He et al., 2019). Songfa et al. (2020) synthesized mesoporous silica supported CuZnO and they showed that antibacterial activities of mesoporous silica supported CuZnO were much better compared to mesoporous silica supported CuO and ZnO (Songfa et al., 2020) because of Cu doped ZnO have smaller band

gap than ZnO, which result in reducing recombination rate of electron-holes that were formed during irradiation of visible light. However, still, the recombination rate of electrons-holes were there because of the electrons in conduction band and holes in valence band of Cu doped ZnO. In addition to this, they synthesized the mesoporous silica particles by hydrothermal method which is very expensive and time consuming method. In this work, CuO-ZnO heterojunction was synthesized on crystalline silica extracted from bagasse ashes by sol-gel method. Here, the combination of the CuO-ZnO doping, or Cu substitute Zn in ZnO or vice versa process may happen in CuO, which leads to reduced recombination rate. The bagasse ashes are low cost, easily synthesized, and non-toxic. The synthesized silica with porosity, unstable surface, and a high adsorption capacity makes them suitable for the growth of nanocomposite and water purification. The porosity nature of silica provides an excellent attachment and adsorption abilities to the nanocomposite (Azmina et al., 2017). Therefore, we found that antibacterial activities of silica-supported CuO/ZnO are better than CuO/ZnO nanocomposites grown without silica substrate.

2. Experimental Methods

2.1. Materials

In this research the raw materials consist of Sugarcane Bagasse Ash (SBA) obtained from Wonji Shewa Sugar Factory (ETHIOPIA), Zinc(II) acetate dihydrate ($Zn(CH_3COO)_2 \cdot 2H_2O$) 98% (Merck), copper(II) sulfate pentahydrate ($CuSO_4 \cdot 5H_2O$) 98% (Merck), ethanol 98%, sodium hydroxide (NaOH) (Merck), filter paper, ethylene glycol ($CH_2OH)_2$), citric acid 10% ($C_6H_8O_7$), Hydrochloric acid (HCl), dimethylsulfoxide (DMSO) and distilled (DI) water. Chemicals used in this experiment were analytical grade and used without extra purification.

2.2. Preparation of Silica from Sugarcane Bagasse Ash

The SBA was calcined in the furnace for 4hrs at 1100°C to remove carbon. Then it was cooled down up to room temperature before taking it out. After that, the ash was washed with 1M HCl to remove extractive minerals and iron composition. The cleaned products were filtered with filter paper named as What-man No 41. Then 20 g solid was treated with 200 mL of 3M NaOH under heating and stirring at 100°C for 90 min.

The mixture was cooled and filtered to remove solid residues. The obtained sodium silicate solution was precipitated using a 1M HCl solution until pH 7 and kept for 24 hrs at 25°C for silica to completely solidify. The slurry was filtered and washed with DI water until it reached neutral Ph. The solids were dried using an oven at 100°C for 24 hrs (Rahman et al., 2016; Mengistu, 2018).

2.3. Synthesis of CuO/ZnO Grown on Silica

Two gram of silica was added to 50 ml of distilled water, 50 ml ethylene glycol, and 8 ml of citric acid and stirred for 30 min. After that 10.649 g of zinc acetate was dissolved into 25 ml of DI water and added to the previous solution drop by drop and stirred vigorously for 1 hr at room temperature. Then, 2.66 g of CuSO₄.5H₂O which dissolved in 25 ml DI water was added again drop by drop and stirred at 60°C for 3 hrs. It was placed in a dark area for 48 hrs. Then, washed with DI water several times, and then washed with ethanol. Finally, the gel was dried at 120°C followed by calcination at 500°C for 4 hrs. (Widiarti et al., 2017). The synthesizing procedures of the bare CuO/ZnO were the same as that of the synthesizing procedures of silica-supported CuO/ZnO except in synthesizing of silica-supported CuO/ZnO need the addition of silica.

3. Results and Discussions

3.1. XRD Analysis

X-Ray Diffraction (XRD) was used to analyze patterns of CuO/ZnO bare and CuO/ZnO grown on crystalline silica as shown on Figure 1.

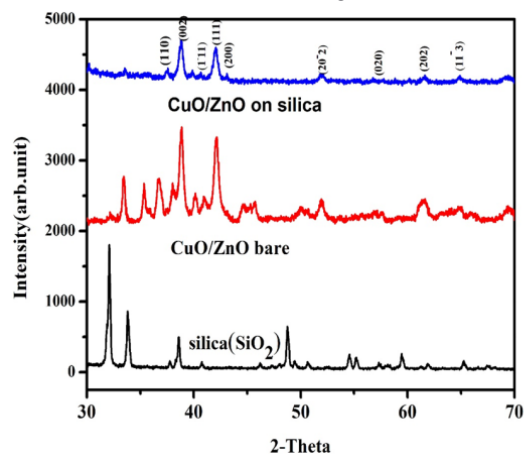


Figure 1: X-ray diffractograms of CuO/ZnO bare, Silica-supported CuO/ZnO supported on silica and silica

The diffraction peak obtained at $2\theta=34.2^\circ, 35.7^\circ, 37^\circ, 38.9^\circ, 41.7^\circ, 48.7^\circ, 53.8^\circ, 58.4^\circ, 61.5^\circ$ with Miller indices, (110), (002), (11 $\bar{1}$), (111), (200), (20 $\bar{1}$), (020), (202), (11 $\bar{3}$). The presence of CuO was identified by comparing with (JCPDS Card No. 48-1548) for 2θ values of 37° and 41.7° and with miller indices (11 $\bar{1}$), and (200) (Li, H, et al., 2016). The high intense peak observed in CuO/ZnO bare indicates high crystalline nature than CuO/ZnO silica supported. Also sharp peaks at (002) and (111) show high crystalline nature of ZnO with hexagonal structure. The crystalline size was calculated from 2θ and FWHM of the (h k l) peaks using Scherer's relation as shown in equation 1 (Hojabri, et al., 2014).

$$D = k\lambda / \beta \cos \theta \dots\dots\dots (1)$$

where, D is crystallite size, K is Shape factor has a typical value of about 0.9, λ is the X-ray wavelength with value 1.54060 nm and β is the line broadening at half the maximum intensity (FWHM), θ is the Bragg angle.

The calculated average crystallite size of the synthesized CuO/ZnO is less than 50 nm because smaller particle size has tremendous effect on the antibacterial activities. For instance, Nandiyanto et al. (2017) reported that smaller crystallite size value has significant effect on the performance of nanocomposites (Nandiyanto et al., 2017). In our case, the calculated average crystallite size of CuO/ZnO bare is 16.3 nm and CuO/ZnO grown on silica is 29.1 nm. Even though, the size of silica supported CuO/ZnO is larger than bare CuO/ZnO, it show better antibacterial activities because it is free from agglomeration as it is confirmed by SEM results. The reason why the XRD peak of silica did not appear in the silica-supported CuO/ZnO is due to the whole surface of silica is covered by CZ nanocomposite.

3.2. Fourier Transform Infrared Spectroscopy (FTIR) Analysis

When infrared light interacts with the substance chemical bonds will stretch, contract and bend. The functional group of samples was recorded beneath the infrared spectroscopy of the wavenumber of 500 cm⁻¹-4000 cm⁻¹. The functional group $\bar{O}H$ of CuO/ZnO on silica and CuO/ZnO bare nanocomposites samples located at wide absorption peaks between 3280 cm⁻¹ – 3650 cm⁻¹ are as shown on Figure 2.

The presence of the $\bar{O}H$ functional group indicates the existence of water absorption on the surface of the

nanocomposite (Saravanak, et al., 2018). The C=O functional group observed at the wavenumber 1650 cm^{-1} , C-O at 1123 cm^{-1} and C-H at 2929 cm^{-1} for both samples. The appearance of C=O, C-O and C-H functional groups is due to the unsuitable decomposition of acetate functional groups present in ZnO precursor. The peaks observed at 790 cm^{-1} may indicate Si-O-Si functional group exists due to silica used as a substrate in the CZ synthesized. The absorption band of metal oxide was below 1000 cm^{-1} due to its inter-atomic vibrations. Strong absorption band in the range $700\text{ cm}^{-1} - 400\text{ cm}^{-1}$ assigned to Cu-O stretching mode (Qiu et al., 2020). Generally, stretching of Zn-O in the ZnO is between 400 cm^{-1} and 531 cm^{-1} which confirmed the wurtzite structure (Widiarti et al., 2017). The absorption peak acquired at 482 cm^{-1} and 460 cm^{-1} for CuO/ZnO bare and CuO/ZnO grown on silica respectively shows the presence of ZnO (stretching Zn-O). The absorption peak observed at 614 cm^{-1} and 545 cm^{-1} were indicating that the presence of Cu-O stretching on CuO/ZnO bare, and CuO/ZnO on silica. Slight shift in peak occurred in the case CuO is may be because of van der Waals force of attraction between the CuO/ZnO and silica.

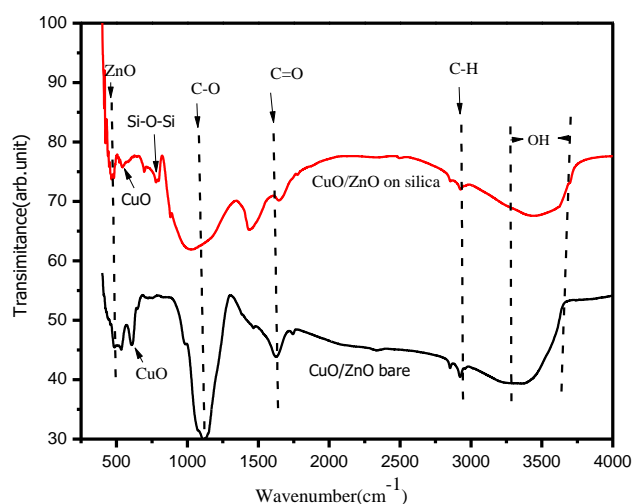


Figure 2: FTIR spectra of CuO/ZnO bare and CuO/ZnO on silica

3.3. Scanning Electron Microscope Analysis

The surface morphology of CuO/ZnO bare and CuO/ZnO on silica were examined using Scanning electron microscope (SEM) and their corresponding EDX are shown in Figure 3. The SEM image clearly displays high clusters of particles which leads to creation of agglomeration in CuO/ZnO bare. This may

be due to addition of CuO to ZnO causes more attraction between particles (Sajjad et al., 2018). In addition to this the surface energy of the particles forced them to stick together to gain stability (Vuong et al., 2016). The morphology of CuO/ZnO on silica is modified because the silica substrate has uniform particle distribution and smooth surface. This allows CuO/ZnO grow easily and prevent agglomeration. The modification of morphology enriches CuO/ZnO to have more active sites for better antibacterial activity. Here, EDX showed that CZ bare contains all expected elements and similarly, silica supported CZ nanocomposites contains all expected elements. In both nanocomposites, the impurities Mo was detected.

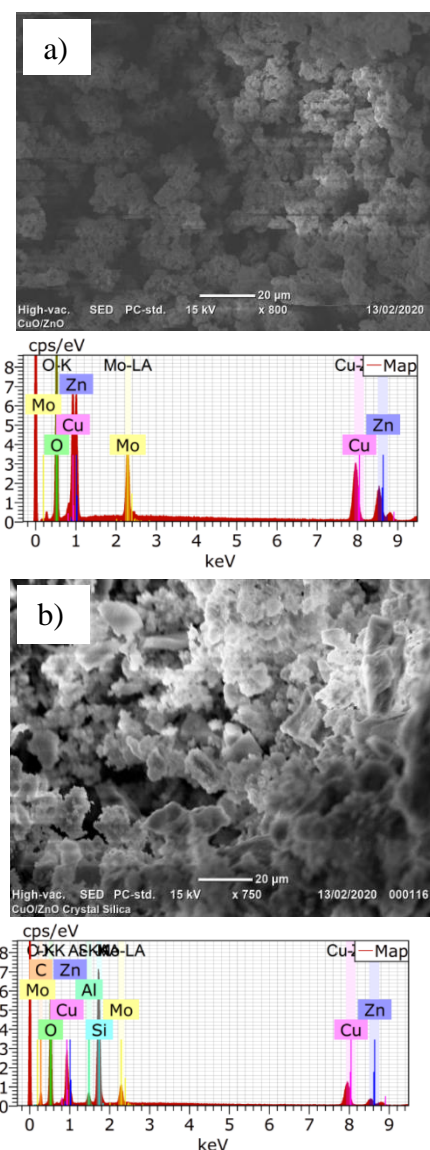


Figure 3: SEM image of (a) CuO/ZnO bare and its EDX, (b) CuO/ZnO grown on silica and its EDX

3.4. Ultraviolet-Visible Spectroscopy Analysis

UV-Vis absorption spectra and Kubelka Munk plot of band gap estimation of CuO-ZnO bare and silica-supported CuO/ZnO nanocomposite were measured as shown in Figure 4. The absorbance measurements were done by using UV-Visible spectroscopy which consists of a light source, collimator, monochromator, and wavelength selector, cuvette for sample solution, a photoelectric detector and a digital display. We dispersed our nanocomposite in DMSO and spread them on thin film glass. The sample solution puts into cuvette first lens transmits a straight beam of light that passes through a monochromator to split it into several component wavelengths. Then, a wavelength slit transmits only the desired wavelengths. After the desired range of wavelength of light passes through the solution of a sample in cuvette, the photometer detects the amount of photons that is absorbed and then absorbance versus wavelength data were displayed on PC.

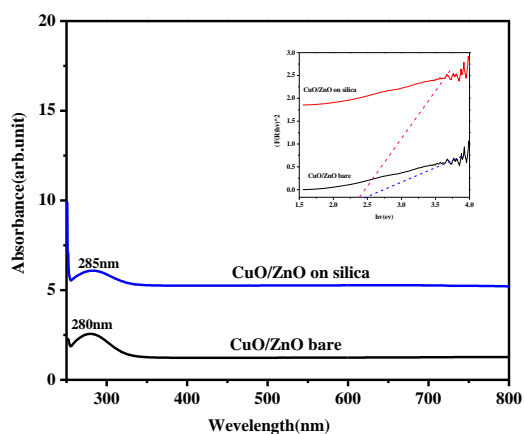


Figure 4: UV-Vis absorption spectra and the Kubelka Munk plot of band gap estimation

As shown in Figure 4, the absorption spectra of CuO/ZnO bare and silica supported CuO/ZnO are nearly the same because their difference is only supporting material i.e. silica has no contribution on the narrowing band gap of CuO/ZnO heterostructure. Therefore, the band gap of the two materials is nearly the same, which leads absorption spectra of the two materials to have insignificant difference. From the Kubelka Munk plot, the band gap of the silica-supported CZ and CZ bare is nearly the same because of aforementioned reasons. Therefore, the band gap of the two materials is nearly the same which lead to same absorption spectra for both nanocomposites. In fact, Jianyu et al. (2015) reported

that the maximum absorption wave length of CuO-ZnO nanocomposite is around 300 nm. Thus, the calculated error bar for CZ bare is 3.4% and 2.5% for silica supported CZ. Therefore, the maximum absorption wavelengths of CZ bare and silica supported CZ nearly the same as that reported by Jianyu et.al. (2015). The maximum absorption wavelengths are 280nm and 285 nm for CuO/ZnO bare and silica-supported CuO/ZnO, respectively. Enhancement of absorption in the UV region was observed in silica-supported CuO/ZnO than CuO/ZnO bare due to reflectance of UV light by silica in the silica-supported CuO/ZnO (Azmina et al., 2017). In addition to this, the agglomeration of CuO/ZnO bare also responsible for the reduction of absorbance in CuO/ZnO bare due to agglomeration leads to large particle size, large particle size mean low particle concentration and low absorbance (Goh et al., 2014).

3.5. Antibacterial Activity Test

The antibacterial test was conducted on both Gram-negative (*Escherichia coli*) bacteria and Gram-positive (*Staphylococcus aureus*) bacteria. The cultural media of bacteria were prepared at Adama Science and Technology University, Biology department. The antibacterial activity test was conducted by the agar well diffusion method. For 24 hrs bacteria were grown in a biochemical incubator. After that both types of bacteria were spread on the agar media by cotton. We measured our nanocomposite on two different weights starting from the most frequently used weight of 15 mg/ml and 20 mg/ml. The measured nanocomposites were dispersed in the DMSO (Dimethyl Sulfoxide) for 30 min. Then, three well were formed on the medium. The prepared nanocomposite solution was added in the drilled part of the media and incubated at 37°C for 24 hrs. The zone of inhibition was measured for 15 mg/ml nanocomposites after 24 hr as shown in Table 1. However, we have faced difficulty on measuring the value of 20 mg/ml nanocomposite due to its high inhibition of the bacteria growth.

From Table 2, we conclude that the inhibition zone of nanocomposite is better in gram-positive (*Staphylococcus aureus*) compared with gram-negative (*Escherichia coli*) bacteria. This is because of Gram-negative bacteria (*Escherichia coli*) typically contain thin cell wall and outer membrane, a layer of the cytoplasmic membrane.

Table 1: Zone of inhibition

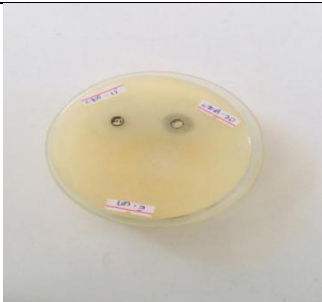
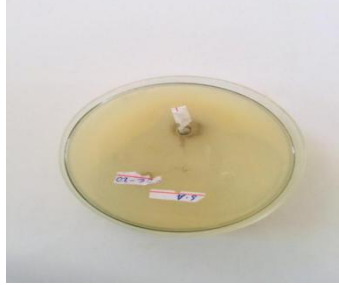
Samples	<i>Staphylococcus aureus</i>	<i>Escherichia coli</i>
CuO/ZnO Bare		
CuO/ZnO grown on crystalline silica		

Table 2: Zone of inhibition values of measured after 24 hrs.

Samples	<i>Staphylococcus aureus</i>	<i>Escherichia coli</i>
CuO/ZnO Bare	25mm	15mm
CuO/ZnO grown on crystalline silica	27mm	17.5mm

This outer membrane resists certain drugs and antibiotics from penetrating the bacteria cell. Gram-positive bacteria contain a thick layer of the cell as well as a layer of the cytoplasmic membrane, which make gram-positive bacteria more susceptible to antibiotics than gram-negative bacteria (Zeng et al., 2013). This is due to Gram-positive bacteria had thick cell wall which leads to absorb nanocomposite highly compared to Gram-negative bacteria (Pasquet et al., 2014).

Antibacterial activity of CuO/ZnO nanocomposite depends on reactive oxygen species, Cu²⁺ and Zn¹⁺ released from the decomposition of CuO/ZnO and concentration of CuO/ZnO. We obtained enhanced antibacterial activity from CuO/ZnO grown on crystalline silica compared to CuO/ZnO bare nanocomposites. This is due to higher amount of Reactive Oxygen Species (ROS) such as superoxide radical anion (O⁻²), hydroxyl radical (·OH), hydrogen peroxide (H₂O₂). The reason why CZ synthesized on silica substrate have high ROS than CZ bare is because of well dispersed states of CuO/ZnO nanocomposite, in

other words, free from agglomeration. In fact, once the nanocomposite agglomerate, the surfaces at which electrons and dissolved oxygen joined was reduced, and vice versa for nanocomposites that are free from agglomeration. Therefore, Silica supported CuO/ZnO nanocomposite has higher free surfaces to generate the ROS than CZ bare. Moreover, as Jan et al. (2019) reported, adding CuO on ZnO introduce more surface defect on CuO/ZnO. The higher surface defect is related to a higher amount of reactive oxygen species (ROS) which in turn leads to higher bacterial inhibition (Jan et al., 2019).

4. Conclusion

In this research, CuO/ZnO bare and CuO/ZnO on silica were successfully synthesized via sol gel method and then characterized with XRD, SEM, FTIR, UV-Vis spectroscope and agar well diffusion method. The average crystal sizes of CuO/ZnO bare is 16.3 nm, and silica-supported CuO/ZnO is 29.1 nm as calculated from XRD data. Moreover, SEM results showed that there was no agglomeration in silica-supported CuO/ZnO due

to the presence of silica. Similarly, FTIR also revealed that values less than 1000 cm^{-1} show the presence of metal oxides. The absorption peaks are observed at 280 nm for CZ-bare and 285 nm for CZ supported on silica. The antibacterial activities of synthesized nanocomposites were investigated on *E. coli* and *S aureus* bacteria. When antibacterial activities of both nanocomposites were tested by using the agar well diffusion method, silica-supported CuO/ZnO showed an inhibit zone of 51% for *Staphylococcus aureus* and 53% for

Escherichia coli compared with that of CuO/ZnO bare. Therefore, silica-supported CuO/ZnO nanocomposite is a promising antibacterial agent because of its low cost, non-toxicity, and good antibacterial properties.

Acknowledgment

The Authors are grateful to the Department of Material Science and Engineering, Adama Science and Technology University for support provided.

Reference

- Ademe, A. S., & Alemayehu, M. (2014). Source and determinants of water pollution in Ethiopia: distributed lag modeling approach. *Intellectual Property Rights: Open Access*.
- Ademiluyi, F. T., Amadi, S. A., & Amakama, N. J. (2009). Adsorption and Treatment of Organic Contaminants using Activated Carbon from Waste Nigerian Bamboo. *Journal of Applied Sciences and Environmental Management*, 13(3).
- Ahmmad, B., Leonard, K., Islam, M. S., Kurawaki, J., Muruganandham, M., Ohkubo, T., & Kuroda, Y. (2013). Green synthesis of mesoporous hematite ($\alpha\text{-Fe}_2\text{O}_3$) nanoparticles and their photocatalytic activity. *Advanced Powder Technology*, 24(1): 160-167.
- Anandan, S., Vinu, A., Mori, T., Gokulakrishnan, N., Srinivasu, P., Murugesan, V., & Ariga, K. (2007). Photocatalytic degradation of 2, 4, 6-trichlorophenol using lanthanum doped ZnO in aqueous suspension. *Catalysis Communications*, 8(9): 1377-1382.
- Azmina, M. S., Nor, R. M., Rafaie, H. A., Razak, N. S. A., Sani, S. F. A., & Osman, Z. (2017). Enhanced photocatalytic activity of ZnO nanoparticles grown on porous silica microparticles. *Applied Nanoscience*, 7(8): 885-892.
- Bandara, J., Hadapangoda, C. C., & Jayasekera, W. G. (2004). TiO₂/MgO composite photocatalyst: the role of MgO in photoinduced charge carrier separation. *Applied Catalysis B: Environmental*, 50(2): 83-88.
- Chauhan, S., Gupta, K. C., Singh, J., & Morar, G. (2015). Purification of drinking water with the application of natural extracts. *Journal of Global Biosciences*, 4(1): 1861-1866.
- Fazal-ur-Rehman, M. (2019). Polluted Water Borne Diseases: Symptoms, Causes, Treatment and Prevention. *Journal of Medicinal and Chemical Sciences*, 2(3): 85-91.
- Goh, E. G., Xu, X., & McCormick, P. G. (2014). Effect of particle size on the UV absorbance of zinc oxide nanoparticles. *Scripta Materialia*, 78: 49-52.
- He, X., Yang, D. P., Zhang, X., Liu, M., Kang, Z., Lin, C., & Luque, R. (2019). Waste eggshell membrane-templated CuO-ZnO nanocomposites with enhanced adsorption, catalysis and antibacterial properties for water purification. *Chemical Engineering Journal*, 369: 621-633.
- Hojabri, A., Hajakbari, F., Soltanpoor, N., & Hedayati, M. S. (2014). Annealing temperature effect on the properties of untreated and treated copper films with oxygen plasma. *Journal of Theoretical and Applied Physics*, 8(3): 132.
- Hopkins, D. R., Weiss, A. J., Roy, S. L., Zingeser, J., & Guagliardo, S. A. J. (2019). Progress Toward Global Eradication of Dracunculiasis-January 2018-June 2019. *Morbidity and Mortality Weekly Report*, 68(43): 979.
- Inyinbor Adejumoke, A., Adebessin Babatunde, O., Oluyori Abimbola, P., Adelani Akande Tabitha, A., Dada Adewumi, O., & Oreofe Toyin, A. (2018). Water pollution: effects, prevention, and climatic impact. *Water Challenges of an Urbanizing World*, 33.
- Jan, T., Azmat, S., Mansoor, Q., Waqas, H. M., Adil, M., Ilyas, S. Z., & Ismail, M. (2019). Superior antibacterial activity of ZnO-CuO nanocomposite synthesized by a chemical Co-precipitation approach. *Microbial pathogenesis*, 134:103579.
- Jianyu, Y., Shendong, Z., Xiaoyong, X., Wenchang, Z., Bing, F. and Jingguo, H. (2015). Photogenerated electron reservoir in hetero-p-n CuO-ZnO nanocomposite device for visible-lightdriven photocatalytic reduction of aqueous Cr(VI). *Journal of Materials Chemistry A*, 2015(3): 1199-1207.
- Li, H., Zhu, L., Xia, M., Jin, N., Luo, K., & Xie, Y. (2016). Synthesis and investigation of novel ZnO-CuO core-shell nanospheres. *Materials Letters*, 174: 99-101.
- Manyasree, D., Peddi, K. M., & Ravikumar, R. (2017). CuO nanoparticles: synthesis, characterization and their bactericidal efficacy. *Int J Appl Pharmaceut*, 9(6): 71-74.
- Mengistu, T. (2018). *Synthesis and Characterization of Zeolite A Using Bagasse Ash, as BioSilica Source for Water Hardness Removal* (Doctoral dissertation, ASTU).

- Mia, R., Selim, M., Shamim, A. M., Chowdhury, M., & Sultana, S. (2019). Review on various types of pollution problem in textile dyeing & printing industries of Bangladesh and recommendation for mitigation. *Journal of Textile Engineering & Fashion Technology*, 5(4): 220-226.
- Montoya-Bautista, C. V., Avella, E., Ramírez-Zamora, R. M., & Schouwenaars, R. (2019). Metallurgical wastes employed as catalysts and photocatalysts for water treatment: a review. *Sustainability*, 11(9): 2470.
- Nabi, B. G. R., Hoveydi, H., Jafari, H. R., Karbasi, A., & Nasrabadi, T. (2006). Application of ozonation in drinking water disinfection based on an environmental management strategy approach using swot method. *Iranian Journal of Environmental Health Science & Engineering*, 3(1): 23-30.
- Nandiyanto, A. B. D., Zaen, R., & Oktiani, R. (2020). Correlation between crystallite size and photocatalytic performance of micrometer-sized monoclinic WO₃ particles. *Arabian Journal of Chemistry*, 13(1): 1283-1296.
- Pasquet, J., Chevalier, Y., Couval, E., Bouvier, D., Noizet, G., Morlière, C., & Bolzinger, M. A. (2014). Antimicrobial activity of zinc oxide particles on five micro-organisms of the Challenge Tests related to their physicochemical properties. *International journal of pharmaceutics*, 460(1-2): 92-100
- Qamar, M. T., Aslam, M., Ismail, I. M., Salah, N., & Hameed, A. (2015). Synthesis, characterization, and sunlight mediated photocatalytic activity of CuO coated ZnO for the removal of nitrophenols. *ACS Applied Materials & Interfaces*, 7(16): 8757-8769.
- Qiu, S., Zhou, H., Shen, Z., Hao, L., Chen, H., & Zhou, X. (2020). Synthesis, characterization, and comparison of antibacterial effects and elucidating the mechanism of ZnO, CuO and CuZnO nanoparticles supported on mesoporous silica SBA-3. *RSC Advances*, 10(5): 2767-2785.
- Rahmat, N., Sabali, M. A., Sandu, A. V., Sahiron, N., & Sandu, I. G. (2016). Study of calcination temperature and concentration of NaOH effect on crystallinity of silica from sugarcane bagasse ash (SCBA). *Rev. Chim.-Bucharest*, 67(9), 1872-1875.
- Sajjad, M., Ullah, I., Khan, M. I., Khan, J., Khan, M. Y., & Qureshi, M. T. (2018). Structural and optical properties of pure and copper doped zinc oxide nanoparticles. *Results in Physics*, 9: 1301-1309.
- Sakib, A. A. M., Masum, S. M., Hoinkis, J., Islam, R., Molla, M., & Islam, A. (2019). Synthesis of CuO/ZnO nanocomposites and their application in photodegradation of toxic textile dye. *Journal of Composites Science*, 3(3): 91.
- Saravanakkumar, D., Abou Oualid, H., Brahmi, Y., Ayeshamariam, A., Karunanaihy, M., Saleem, A. M., & Jayachandran, M. (2019). Synthesis and characterization of CuO/ZnO/CNTs thin films on copper substrate and its photocatalytic applications. *OpenNano*, 4: 100025.
- Saravanakkumar, D., Sivaranjani, S., Kaviyarasu, K., Ayeshamariam, A., Ravikumar, B., Pandiarajan, S., & Maaza, M. (2018). Synthesis and characterization of ZnO–CuO nanocomposites powder by modified perfume spray pyrolysis method and its antimicrobial investigation. *Journal of Semiconductors*, 39(3): 033001.
- Sharma, S., & Bhattacharya, A. (2017). Drinking water contamination and treatment techniques. *Applied Water Science*, 7(3): 1043-1067.
- Sherly, E. D., Vijaya, J. J., & Kennedy, L. J. (2015). Visible-light-induced photocatalytic performances of ZnO–CuO nanocomposites for degradation of 2, 4-dichlorophenol. *Chinese Journal of Catalysis*, 36(8): 1263-1272.
- Shirzadi, A., & Nezamzadeh-Ejhi, A. (2016). Enhanced photocatalytic activity of supported CuO–ZnO semiconductors towards the photodegradation of mefenamic acid aqueous solution as a semi real sample. *Journal of Molecular Catalysis A: Chemical*, 411: 222-229.
- Sun, J. H., Dong, S. Y., Wang, Y. K., & Sun, S. P. (2009). Preparation and photocatalytic property of a novel dumbbell-shaped ZnO microcrystal photocatalyst. *Journal of Hazardous Materials*, 172(2-3): 1520-1526.
- Vuong, N. M., Chinh, N. D., Huy, B. T., & Lee, Y. I. (2016). CuO-decorated ZnO hierarchical nanostructures as efficient and established sensing materials for H₂S gas sensors. *Scientific reports*, 6(1): 1-13.
- Widiarti, N., Sae, J. K., & Wahyuni, S. (2017). Synthesis CuO-ZnO nanocomposite and its application as an antibacterial agent. In *IOP Conference Series: Materials Science and Engineering*, 172(1): p. 012036.
- Zeng, X., & Lin, J. (2013). Beta-lactamase induction and cell wall metabolism in Gram-negative bacteria. *Frontiers in microbiology*, 4: 128.
- Zioui, D., Tigrine, Z., Aburideh, H., Hout, S., Abbas, M., & Merzouk, N. K. (2015). Membrane Technology for water treatment applications. *International Journal of Chemical and Environmental Engineering*, 6(3).